ITS-90 TRACEABLE CALIBRATION OF RADIOMETERS USING WIRE/THIN-FILM THERMOCOUPLES IN THE NIST RTP TOOL: EXPERIMENTAL PROCEDURES AND RESULTS

C.W. Meyer, D.W. Allen, D.P. DeWitt, K.G. Kreider, F.L. Lovas, and B.K. Tsai

We have performed comparisons in a rapid thermal processing (RTP) chamber of the spectral radiance temperature T_λ of a silicon wafer measured by light-pipe radiation thermometers (LPRTs) with the true temperature T of the wafer measured by high-accuracy wire/thin-film thermocouple combinations (TCs). The results have been used for *in situ* calibrations of the LPRTs against the TCs, which have calibrations traceable to the International Temperature Scale of 1990 (ITS-90). The TCs can determine temperatures with an uncertainty of less than 1 °C (all uncertainties referred to here are 1 σ). The comparisons of T_λ with T were made after the wafer reached a steady-state temperature under constant heating. The uncertainty of the comparisons was less than 1.5 °C over the temperature range 650 °C < T < 900 °C. In the RTP tool of the National Institute of Standards and Technology (NIST), the cavity underneath the wafer is surrounded with shields of high reflectivity, which minimizes stray radiation and raises the wafer effective emissivity ε_{eff}. The comparisons of T_λ with T at the center of the wafer show that with the appropriate shield reflectivity and wafer/shield spacing, $T - T_\lambda \leq (3.0 \pm 1.5)$ °C for T < 900 °C. The measured temperature differences indicate that $\varepsilon_{eff} \approx 0.98$.

INTRODUCTION

Accurate temperature measurement of silicon wafers during rapid thermal processing (RTP) is of critical importance for manufacturing reliable, high quality devices. To meet the Semiconductor Industry Association roadmap [1], the requirement is for an RTP temperature measurement uncertainty of less than 2 °C and temperature measurement reproducibility of better than 0.25 °C at 1000 °C. Because of their non-intrusiveness, light-pipe radiation thermometers (LPRTs) are the preferred sensor system but are subjected to uncertainties associated with wafer emissivities and stray radiation. [2] Ripple pyrometry [3] and emissivity-free pyrometry [4] have been developed to increase the temperature measurement accuracy of LPRTs by minimizing these uncertainties, but as of the present, the reliability of these methods has not been established by a rigorous uncertainty analysis. Furthermore, these methods do not provide traceability to the International Temperature Scale of 1990 (ITS-90) [5].

In this paper we discuss two different methods that have been used to increase the accuracy of radiation thermometry in the RTP tool of the National Institute of Standards and Technology (NIST). The first method is *in situ* calibration of LPRTs against wire/thin-film thermocouple combinations with traceability to the ITS-90. The second is insertion of cold reflective shields in appropriate locations to provide an enclosure underneath the wafer [2,5]. This enclosure reduces stray radiation and improves wafer temperature uniformity. It also increases the effective emissivity ε_{eff} of the wafer, which is determined by the radiative properties of the wafer and chamber and by the chamber geometry. A companion paper [6] explains how the enclosure increases ε_{eff} and also presents a model that determines ε_{eff} by characterizing the radiation environment.

In situ calibration of LPRTs against wire thermocouples mounted on a silicon wafer in an RTP chamber has been used for many years. Wire thermocouples, however, can have unsatisfactorily large uncertainties because they conduct heat well, thereby serving as a heat sink that lowers the temperature in the vicinity of the thermocouple junction. [7] The amount of this decrease is estimated to be between 1 °C and 20 °C [7], and this adds considerably to the uncertainty the LPRT calibration. Thin-film thermocouples [8-10] can provide an accurate measurement of the wafer temperature in a location of interest while making a negligible thermal perturbation on the wafer at that location. They measure the temperature difference between the location of interest and another location on the periphery of the wafer, where high-accuracy platinum-palladium wire thermocouples are welded. The perturbation of the thin films on the wafer is

negligible because they have a minimal thermal conductivity across their length, and their measurement accuracy is high because they have a strong thermal connection to the wafer. By using the combination of thin-film thermocouples and Pt/Pd thermocouples, the temperature of a location of interest on the wafer can be measured with an accuracy of a few tenths of a degree Celsius [9].

The cold reflective shields surrounding the enclosure underneath the wafer are used to block stray radiation from the cavity and improves temperature uniformity of the wafer. Increasing ε_{eff} by insertion of the shields [6] lowers the temperature difference ΔT_λ between the true wafer temperature T and the spectral radiance temperature T_λ measured by the LPRT, as shown by the temperature measurement equation [11],

$$\frac{1}{T} = \frac{1}{T_\lambda} + \frac{\lambda}{c_2} \cdot \ln \varepsilon_{eff}, \qquad [1]$$

where λ is the wavelength and c_2 is the second radiation constant. Increasing ε_{eff} also lowers the uncertainty in LPRT measurements due to the variations in wafer emissivity ε. When reflective shields are used, variations in ε result in much smaller variations in ΔT_λ.

THERMOCOUPLE-INSTRUMENTED WAFER

Figure 1 shows the design of the 200 mm thermocouple-instrumented wafer. A detailed description of the design may be found in [8]. The wafer contained four rhodium-platinum thin-film thermocouples. The thin films were sputter deposited on oxidized silicon wafers using physical masks for the 0.5-µm thick metal films of 99.99 % Pt and 99.95 % Rh, and the films were bonded to the SiO_2 with sputter-deposited Ti. The four junctions were labeled 7, 9, 10, and 12 as shown. Platinum wires of diameter 0.1 mm and length 3 cm were welded to all weld pads, and palladium wires of diameter 0.1 mm and length 3 cm were welded to pads 8 and 11 as shown. Platinum and palladium wires of diameter 0.25 mm and length 0.7 m were then butt-welded to their respective 0.1 mm wires. The Pt thin films are shown in the figure as solid lines and the Rh thin films are shown as dashed lines. The cold junctions of the wire thermocouples were attached to a terminal strip outside the RTP chamber whose temperature (≈21 °C) was measured by a thermistor calibrated by the NIST Thermometry Group with an uncertainty (k=2) of 2.4 mK. The two wire thermocouples measured the temperature difference between the terminal strip and their hot junctions at weld pads 8 and 11. Thin film thermocouples 7 and 9 measured the temperature difference between their junctions and weld pad 8. Similarly, thin film thermocouples 10 and 12 measured the temperature difference between their junctions and weld pad 11. The wafer experienced problems with delamination of weld pad 8 after it went through a couple of thermal cycles. Therefore, only those measurements made with junctions 10, 11 and 12 are presented in this paper.

The LPRT targets, which are shown in Fig. 1, were labeled 1, 3 and 4. Target 1 was located 1.6 cm from thermocouple junctions 9 and 10 in order to avoid affecting the emissivity of the wafer over the LPRT target area. Targets 1 and 3 were located 0.5 cm from junctions 7 and 12, respectively.

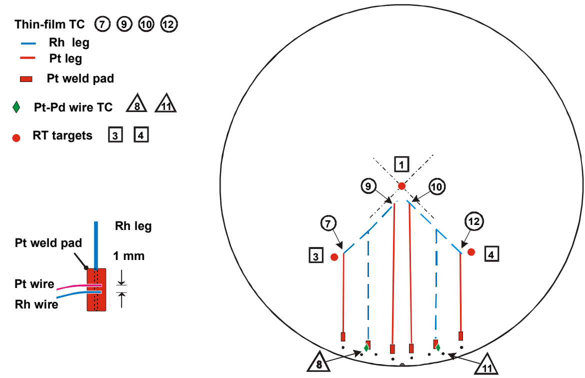

Figure 1. NIST thermocouple-instrumented wafer.

The Pt/Pd wire thermocouples were made from special lots of Pt and Pd wire that had been calibrated by the Thermometry Group of NIST with an uncertainty of 0.1 °C (k=2). The wires were annealed using the procedure describe in [12] and using the Pt/Pd reference functions given in [13]. The thin-film thermocouples were calibrated using the procedure described in [9]. For the temperature differences measured across the thin films on the wafer (< 9 °C), the uncertainty of the thin-film thermocouple calibrations is estimated to be 0.3 °C (k=2).

RTP CHAMBER

The RTP chamber shown in Figure 2 was made of stainless steel and had a height of 8.7 cm, hexagonal sides of length 18.0 cm, and a top composed of a quartz plate of thickness 6 mm. The chamber was purged with 99.9% pure nitrogen gas, which flowed

from three inlets on the sidewalls and through an outlet on the bottom as shown. The oxygen content of the gas in the chamber was monitored with an oxygen analyzer and was kept below 150 ppm whenever the wafer was heated. Heating was produced by an array of 24 2 kW quartz-halogen lamps located 15.0 cm above the chamber. The lamps were surrounded on the top and sides by a gold-plated lamp housing with a hexagonal geometry, which reflected stray radiation down into the chamber. The wafer, which was supported by three 2-mm diameter alumina rods, was located approximately 3.6 cm below the quartz plate.

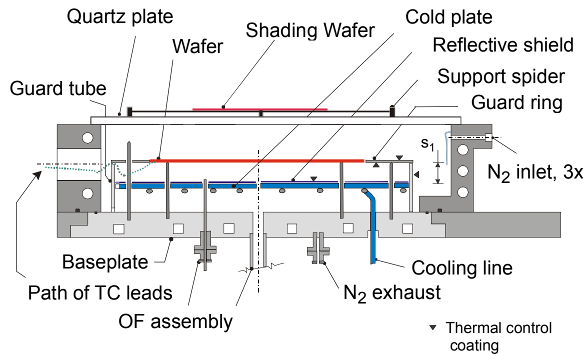

Figure 2. The NIST RTP Chamber

Underneath the wafer was located a 26.7 cm diameter water-cooled copper plate with grooves machined in it to allow it to function as a vacuum chuck. Atop the copper plate was a 1-mm thick brass reflective shield of the same diameter, which was held tight against the copper plate by the applied vacuum. Two reflective shields were made for use with the RTP chamber; the first was sandblasted to provide diffuse reflection and the second was lapped and polished to provide specular reflection, and both were coated with gold to increase their reflectance. Total hemispherical reflectance measurements of the two shields were performed by the NIST Optical Temperature and Source Group using the techniques described in [14]. The reflectance of the diffuse shield was $\rho = 0.799$, and that of the specular shield was $\rho = 0.993$. Five holes were drilled vertically through the copper plate for insertion of the LPRTs. One hole of diameter 4 mm was in the center of the plate and the other four were of diameter 7 mm and located at a radius of 5.4 cm from the center of the plate and at equal angles from each other. The bottom reflective shields had similar holes, except that all holes for LPRTs in the diffuse shield were of diameter 4 mm. In addition to the holes described above, three 2.2 mm diameter holes were drilled through the copper plate and reflective shields at a radius of 7.5 cm and at equal angles for the insertion of the alumina rods supporting the wafer.

The copper plate was surrounded by a 5 mm thick quartz guard tube with an inner diameter of 26.9 cm and height 4.5 cm as shown in the figure. The guard tube was coated on the outside with platinum. On top of the guard tube rested a 1-mm thick quartz guard ring with an outer diameter of 30 cm and inner diameter of 20.2 cm as shown; this ring was coated with platinum on the bottom side. This design provided an enclosure underneath the wafer that was almost completely shielded from stray radiation and which was surrounded on the top and sides by platinum-coated reflective shields and on the bottom by a gold-coated reflective shield.

By supporting the wafer with rods of different length, the spacing between the wafer and the bottom reflective shield could be adjusted. Copper spacers were placed underneath the guard tube when necessary to raise the height of the guard ring into alignment with the wafer. The purpose of making the wafer/shield spacing was allow study of the dependence of ε_{eff} on this parameter, providing data to verify models being developed to characterize the reflective enclosure [6].

When the RTP chamber was first used, it was found that radial temperature gradients existed on the calibration wafer under steady heating such that the center of the wafer was 50 °C higher than the periphery when the wafer was above 600 °C. To minimize these gradients, a silicon shading wafer was placed directly above the calibration wafer. After several trials, it was found that gradients were minimal when the shading wafer was 12.7 cm in diameter and was placed above the quartz plate as shown in Fig. 2. The shading wafer was supported by a set of horizontal and vertical alumina rods joined together by boron nitride connectors. When using the shading wafer, temperature variations on the wafer (as determined by temperature differences measured across the thin-film thermocouples) were less than 9 °C.

INSTRUMENTS AND DATA ACQUISITION

The LPRTs used were commercially made and consisted of three 2-mm diameter sapphire light pipes connected to a 0.95-µm wavelength radiometer with 1-mm diameter optical fibers. The light pipes were surrounded by sapphire sheaths of outer diameter 3.8 mm. They were calibrated against a sodium heat-pipe blackbody source [14] at 750 °C, 800 °C,

850 °C, and 900 °C. The temperature of the blackbody was measured with a Au/Pt thermocouple, which had been calibrated with an uncertainty (k=2) of 0.01 °C. The calibration was performed by setting the LPRT sensor factor when the blackbody was at 900 °C. At the other temperatures, the difference between the blackbody temperature and that on the LPRT measurement display was recorded to complete the calibration. During the calibration, each light pipe was separately inserted 7 cm into the blackbody. Once the temperature reading stabilized (<10 s), the calibration measurement was immediately made; this prevented the light pipes from heating significantly, which can cause drifts in their display reading [14]. When transporting the calibrated LPRTs from the calibration laboratory to the RTP chamber, the optical fiber cables were not disconnected from the control unit, thereby maintaining their blackbody calibration to within 0.1 °C. The LPRTs were placed in the RTP chamber such that their tips were at the same height as the bottom reflective shield.

The emf across each thermocouples was measured using a multimeter with a resolution of 0.01 μV and an accuracy of 2.5 ppm. The same multimeter was used to measure the resistance of the thermister measuring the temperature of the thermocouple cold junctions. A scanner was used to switch between the different thermocouples and the thermister. Data acquisition was automated by a personal computer interfaced with the LPRTs, scanner, and multimeter.

The *in situ* calibration measurements were made under steady heating at various power levels. Once the lamp power was set, temperatures measured by the thermocouples and blackbody-calibrated LPRTs were recorded as a function of time. The time interval between each thermocouple measurements was 5 s, and that between measurement sets was 45 s. For each power level, measurements continued until a steady-state temperature was reached. Only the final steady-state values were used for the *in situ* calibration. Final wafer temperatures ranged between 650 °C and 920 °C. Measurements were performed using both diffuse and specular shields. Wafer/shield spacings of 6 mm, 9 mm, 12.5 mm, and 15.5 mm were used.

MEASUREMENT UNCERTAINTIES

The measurement uncertainties are given below in Table 1. The coverage factor for the uncertainties is k=1. The total uncertainty for the thermocouple-LPRT comparisons includes all items in the table, but that for the *in situ* LPRT calibration against the thermocouples excludes the blackbody/LPRT calibration uncertainty.

The dominant uncertainty arises from the separation between the thin-film thermocouple junctions and the center of the LPRT target. During the calibration measurements, the temperature difference between junctions 10 and 12 was almost always less than 5 °C, and their physical separation was 3.8 cm. The uncertainty estimate of 2.0 °C was based on the assumption of a uniform temperature gradient between junction 12 and the center. However, no correction for temperature gradients was ever applied to the calibration measurements. Other measurement uncertainties were from temperature fluctuations and long-term temperature drift of the wafer while in steady state, thermocouple calibration uncertainties [9,9], LPRT calibration uncertainties, and instrument uncertainties for temperature measurement with the thermocouples and LPRTs.

Table 1. Measurement Uncertainties, where each uncertainty u is given with a coverage factor of k=1.

Item	u/°C
Thermocouple calibrations	0.3
Thermocouple emf measurements	0.1
LPRT calibrations	0.2
LPRT measurements	0.1
Wafer temperature fluctuations	0.4
Wafer Temperature drift	0.1
Junction/target temp. difference	2.0
Total: *in situ* LPRT calibration	2.1
Total: TC/LPRT comparison	2.1

RESULTS

Figure 3a shows a comparison between the temperatures measured by the thermocouple combination (T_{tc}) and those measured by the LPRT (T_λ). The measurements were made near the center of the wafer and with a wafer/shield spacing of 12.5 mm. Results using the diffuse shield are shown as diamonds and results using the specular shield are shown as squares. The values of T_{tc} - T_λ for the specular shield are all within 3 °C; this demonstrates that with such a chamber environment, the blackbody-calibrated LPRT will read the correct temperature to within this amount. The values of T_{tc} - T_λ for the diffuse shield are larger; this is expected, because the reflectance of the specular

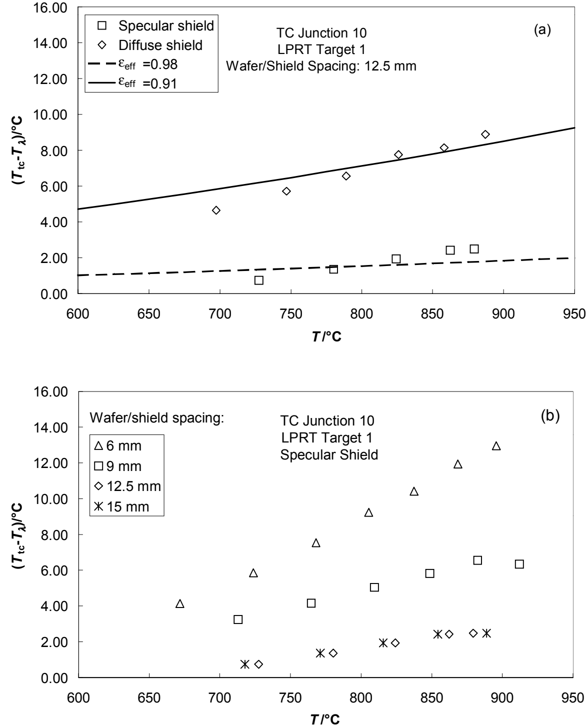

Figure 3. Comparisons between temperatures measured by a wire/thin-film thermocouple combination (T_{tc}) and temperatures measured by an LPRT (T_λ). The temperatures were measured near the center of the wafer. In (a) the wafer/shield spacing is 12.5 mm and the results with a gold specular shield (reflectance $\rho = 0.993$) and a gold diffuse shield ($\rho = 0.799$) are shown. The curves show the values that would be expected for effective emissivities of 0.91 and 0.98 using Eq. 1. In (b) the specular shield is used, and results with four different wafer/shield spacings are shown.

shield ($\rho = 0.993$) is higher than that of the diffuse shield. ($\rho = 0.799$), and so its value for ε_{eff} is expected to be higher [6]. For both the specular and diffuse shields, the temperature-measurement accuracy of the LPRT will be improved by *in situ* calibration, which corrects for the T_{tc}-T_λ values observed.

The curves shown represent the temperature difference expected for effective emissivities of 0.91 and 0.98 using Eq. 1. The emissivity values were chosen so that the curves would best fit the data. The slope of the data in Fig. 3a is clearly larger than that of the curves, showing that ε_{eff} for the wafer decreases with temperature. This temperature dependence of ε_{eff} is surprising, since the emissivity of the wafer ($\varepsilon \cong 0.65$) has a very low temperature dependence over this temperature range. A possible reason is that the temperatures of the guard ring and guard tube increase as the wafer temperature increases. This temperature dependence may make the emissivity enhancement ratio $\varepsilon_{eff}/\varepsilon$ temperature dependent.

Figure 3b shows the effects of changing the wafer/shield spacing on T_{tc}-T_λ. For this plot, the specular shield was used. While the results for spacings of 12.5 mm and 15.5 mm are identical to within the resolution of the measurements, the values for T_{tc}-T_λ increase as the spacing is decreased from 12.5 mm to 6 mm. This effect can be explained by the optical perturbation on ε_{eff} of the LPRT target area caused by the presence of the light pipe, which has a much smaller reflectance ($\rho = 0.075$) than the shield. The light pipe occupies a larger solid angle of the field-of-view of a point on the target area as the wafer/shield spacing decreases. Because of this effect, an *in situ* calibration should be performed with the same spacing as in the application.

In Figure 4, the values of $\Delta T_\lambda \equiv T_{tc}$-$T_\lambda$ for junction 10 and target 1 are subtracted from those for junction 12 and target 4. Here, the wafer/shield spacing is 12.5 mm. For the diffuse shield, the difference is less than 0.4 °C, showing agreement to within the uncertainties between these two measurements. However, for the specular shield, the difference was as large as 7 °C. This large difference can be explained by the larger size hole surrounding light pipe 4 in the specular shield. The diameter of this hole was 7 mm, while that for the center hole was 4 mm. For the diffuse shield, all LPRT holes were 4 mm. The larger hole size for light pipe 4 in the specular shield increased the optical perturbation on the LPRT target area caused by the presence of the light pipe, thereby decreasing ε_{eff} in that location and increasing ΔT_λ [6]. The results of Fig. 3b and Fig. 4 demonstrate the large optical perturbation that the presence of the LPRT can have on ε_{eff} of the wafer target area, and how that perturbation can be minimized.

SUMMARY

We have performed *in situ* calibrations of LPRTs against ITS-90 wire/thin-film thermocouple combinations with ITS-90 traceability in an RTP chamber. The chamber was designed with an optically enhanced environment involving cold reflective shields that blocked stray radiation and increased the effective emissivity of the wafer.

Calibrations were performed with an uncertainty (k=1) of 2.1 °C, where the dominant uncertainty was due to the separation between the thermocouple junction and the LPRT target. When shield placed underneath the wafer was specularly reflective, the hole surrounding the LPRTs was 4 mm and the wafer/shield spacing was 12.5 mm, the spectral radiance temperatures measured by the blackbody-calibrated LPRT agreed with the temperatures measured by the thermocouples to within 3 °C; this corresponds to an effective emissivity of $\varepsilon_{eff} \approx 0.98$. While *in situ* calibration of LPRTs alone is very useful, radiation modeling efforts are needed to improve confidence for the calibrations and to understand the effects of shield reflectance and the optical perturbation of the LPRTs on values of $T_{tc} - T_{\lambda}$.

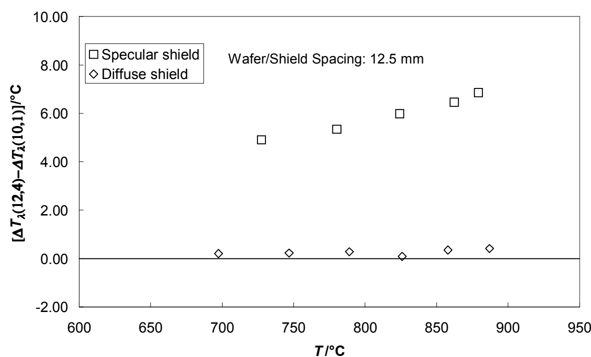

Figure 4. Difference between the values of $\Delta T_{\lambda} \equiv T_{tc} - T_{\lambda}$ for junction 10/target 1 (at center of wafer) and those for junction 12/ target 4 (at radius of 5 cm). The wafer/shield spacing is 12.5 mm. Results with both reflective shields are shown.

REFERENCES

[1] SIA Semiconductor Industry Association, The National Technology Roadmap for Semiconductors, 3rd edition, Semiconductor Industry Association, San Jose, 1997

[2] D.P. DeWitt, F.Y. Sorrell, and J.K. Elliott, "Temperature Measurement Issues in Rapid Thermal Processing", Mat. Res. Soc. Proc.

[3] A.T. Fiory and A.K. Nanda, "Ripple Pyrometry for Rapid Thermal Annealing", Mat. Res. Soc. Proc. Vol. 342, 1994

[4] J. Hebb and A. Shajii, "Temperature Measurement, Uniformity, and Control in a Furnace-Based RTP System", to be published in the proceedings of the Spring 1999 Meeting of the Electrochemical Society.

[5] H. Preston-Thomas, Metrologia, vol. 27 (1990), p. 3

[6] B.K. Tsai and D.P. DeWitt, "ITS-90 Traceable Calibration of Radiometers Using Wire/Thin-film Thermocouples in the NIST RTP Tool: Effective Emissivity Modeling", Proceedings of this conference.

[7] P.J. Vandenabeele and W. Renken, "Study of Relative Accuracy, Repeatability and Lifetime of Thermocouple Instrumented Calibration Wafers for RTP," Mat. Res. Soc. Proc.

[8] K.G. Kreider, F. DiMeo, Sensors and Actuators, vol. A69 (1998), p. 46

[9] K.G. Kreider, D.C. Ripple, and D.P. DeWitt, "Determination of the Seebeck Coefficient of Thin-film Thermocouple*s*," in Proceedings of 44th International Instrumentation Symposium, ISA, 1998

[10] K.G. Kreider and G. Gillian, "Thin-Film Calibration Wafer Materials for RTP Temperature Measurement", Proceedings of this conference.

[11] D.P. DeWitt, G.D. Nutter, Theory & Practice of Radiation Thermometry, 1st edition, John Wiley & Sons, Inc. , New York, 1988

[12] G.W. Burns and D.C. Ripple, "Techniques for Fabricating and Annealing Pt/Pd Thermocouples for Accurate Measurements in the Range 0 °C to 1300 °C," in Proceedings of 6th International. Symposium On Temperature and Thermal Measurements in Industry, TEMPMEKO '96, 1996

[13] G.W. Burns, D.C. Ripple, and M. Battuello, Metrologia, vol. 35 (1998), p. 76

[14] P.Y. Barnes, E.A. Early, and A.C. Parr, Spectral Reflectance, NIST SP250-48, 1998

[15] F.J. Lovas, B.K. Tsai, and C.E. Gibson, "Meeting RTP Temperature Accuracy Requirements: Measurement and Calibrations at NIST", Mat. Res. Soc. Proc., Vol. 525, 1998